DMD #48678

Characterization of Differential Cocaine Metabolism in Mouse and Rat through Metabolomics-guided Metabolite Profiling

Dan Yao, Xiaolei Shi, Lei Wang, Blake A. Gosnell, Chi Chen

Department of Food Science and Nutrition, University of Minnesota, St. Paul, MN 55108

1

DMD #48678

Running title: Cocaine metabolism and hepatotoxicity

Correspondence: Dr. Chi Chen, Department of Food Science and Nutrition, University of Minnesota, 1334 Eckles Avenue, 225 FScN, St. Paul, MN 55108, Tel.: 612-624-7704; Fax: 612-625-5272; Email: chichen@umn.edu

Abbreviations: CIH, cocaine-induced hepatotoxicity; ALT, alanine aminotransferase; P450, cytochrome P450; FMO, flavin-containing monooxygenases; i.p., intraperitoneal; NHNC, *N*-hydroxynorcocaine; UDPG, uridine 5'-diphosphoglucose; NADPH, β-Nicotinamide adenine dinucleotide phosphate; PCA, principal components analysis; RT, retention time; LC-MS, liquid chromatography-mass spectrometry; UPLC, ultra-performance liquid chromatography; TOF-MS, time-of-flight mass spectrometry; MS/MS; tandem MS; ppm, part per million; MLM, mouse liver microsomes; RLM, rat liver microsomes; HLM, human liver microsomes.

Number of text page: 18

Number of table: 1

Number of figures: 6 (plus 1 supplemental figure)

Number of references: 52

Number of words in the Abstract: 250

Number of words in the Introduction: 643

Number of words in the Discussion: 1318

DMD #48678

Abstract

Rodent animal models have been widely used for studying neurological and toxicological events associated with cocaine abuse. It is known that the mouse is more susceptible to cocaine-induced hepatotoxicity (CIH) than the rat. However, the causes behind this species-dependent sensitivity to cocaine have not been elucidated. In this study, cocaine metabolism in the mouse and rat was characterized through LC-MS-based metabolomic analysis of urine samples, and were further compared through calculating the relative abundance of individual cocaine metabolites. The results showed that the levels of benzoylecgonine, a major cocaine metabolite from ester hydrolysis, were comparable in the urine from the mice and rats treated with the same dose of cocaine. However, the levels of the cocaine metabolites from oxidative metabolism, such as *N*-hydroxybenzoylnorecgonine and hydroxybenzoylecgonine, differed dramatically between the two species, indicating species-dependent cocaine metabolism. Subsequent structural analysis through accurate mass analysis and LC-MS/MS fragmentation revealed that *N*-oxidation reactions, including *N*-demethylation and *N*-hydroxylation, are preferred metabolic routes in the mouse, while extensive aryl hydroxylation reactions occur in the rat. Through stable isotope tracing and *in vitro* enzyme reactions, a mouse-specific α-glucoside of *N*-hydroxybenzoylnorecgonine and a group of aryl hydroxy glucuronides high in the rat were identified and structurally elucidated. The differences in the *in vivo* oxidative metabolism of cocaine between the two rodent species were confirmed by the *in vitro* microsomal incubations. Chemical inhibition of P450 enzymes further revealed that different P450-mediated oxidative reactions in the ecgonine and benzoic acid moieties of cocaine contribute to the species-dependent biotransformation of cocaine.

Introduction

Besides neurological and cardiovascular toxicities (Lason, 2001; Knuepfer, 2003; Nutt et al., 2007), cocaine abuse also causes liver injury (Kloss et al., 1984). Detrimental effects of cocaine on the liver have been proven clinically since many chronic cocaine users have higher serum transaminase activities (Marks and Chapple, 1967), and many cases of cocaine-related fatality have been attributed to the cocaine-induced hepatic necrosis (Perino et al., 1987; Kanel et al., 1990; Wanless et al., 1990). In accordance with the clinical observations in humans, cocaine-induced hepatotoxicity (CIH) has been confirmed and established in experimental animal models (Shuster et al., 1988). Mechanistic investigations using these animal models and *in vitro* assays have yielded insights on the initiation and development of CIH. The essential roles of cocaine metabolism in its toxicity, especially the roles of the metabolic activation of cocaine and its metabolites, have been indicated in these studies (Boelsterli and Goldlin, 1991). Among defined pathways of cocaine metabolism, the ester hydrolysis reactions mainly produce non-toxic metabolites, including benzoylecgonine, ecgonine methyl ester, and ecgonine (Thompson et al., 1979), and the hydroxylation of benzoic acid moiety to form a series of aryl hydroxy metabolites facilitates the excretion of cocaine (Smith, 1984; Smith et al., 1984). Metabolic activation of cocaine is through the *N*-oxidation reactions on tropane nitrogen, which are the *N*-demethylation and *N*-hydroxylation reactions catalyzed by cytochrome P450 (P450) and flavin-containing monooxygenases (FMO) (Kloss et al., 1982; Kloss et al., 1983). It has been shown that the metabolites formed by these bioactivation reactions, including norcocaine, *N*-hydroxynorcocaine, and norcocaine nitroxide, are more hepatotoxic than cocaine itself (Thompson et al., 1979; Ndikum-Moffor et al., 1998). Many observed cytotoxic events in cocaine overdose, including covalent binding to proteins, glutathione depletion, and lipid peroxidation, have been defined as

the direct consequences of forming these reactive metabolites (Evans, 1983; Kloss et al., 1983; Masini et al., 1997). The development of CIH is likely due to multiple downstream events, such as the disruption of normal function of mitochondria and other intracellular organelles, the dysregulation of signaling pathways in cell death and survival, and the necrosis and apoptosis of hepatocytes (Gottfried et al., 1986; Shuster et al., 1988; Powers et al., 1992).

An important observation on CIH is that the susceptibility to cocaine is species-, strain-, and sex-dependent (Evans and Harbison, 1978; Thompson et al., 1984; Boyer et al., 1988). Rodents, mainly mouse and rat, have been widely used for examining various pathophysiologival effects of cocaine, including CIH (Lakoski et al., 1992). Compared to the cocaine-naïve rat, the cocaine-naïve mouse is generally much more vulnerable to CIH (Mehanny and Abdel-Rahman, 1991; Powers et al., 1992). Cocaine metabolism has been considered as a major factor underlying the different susceptibility to CIH (Roberts et al., 1992). Currently available data from animal and *in vitro* studies have shown that both mouse and rat are capable of converting cocaine to its reactive metabolites (Misra et al., 1979; Shuster et al., 1983; Toennes et al., 2003). However, due to the lack of detailed comparison of cocaine metabolism between the mouse and rat, the correlation between cocaine metabolism and species-dependent susceptibility to CIH has not been established yet.

Owing to the advances in analytical instrumentation and chemometric computation, metabolomics has become an effective tool to examine xenobiotic metabolism as well as the associated metabolic effects. A clear advantage of this approach is that the multivariate data analysis in metabolomics rationalizes the identification of xenobiotic metabolites and facilitates the analysis of metabolic pathways (Nicholson et al., 2002; Chen et al., 2007a). A recent metabolomics-based study has revealed the changes in tryptophan and purine metabolism after

cocaine addiction (Patkar et al., 2009). In this study, cocaine metabolism in the mouse and rat was investigated by metabolomics-guided metabolite profiling, and the identities of novel cocaine metabolites and the roles of P450 in species-dependent cocaine metabolism were examined by stable isotope tracing and chemical inhibition.

Materials and Methods

Reagents. Cocaine HCl, [$^2H_5$-*phenyl*]-cocaine, [$^2H_3$-*N-methyl*]-cocaine HCl, *N*-norcocaine, cocaine *N*-oxide HCl, benzoylecgonine, benzoylnorecgonine HCl, and ecgonine methyl ester HCl were kindly supplied by RTI international (Research Triangle Park, NC) via the National Institute on Drug Abuse Drug Supply Program. HPLC-grade water, acetonitrile, formic acid, sulfaphenazole, orphenadrine, α-glucosidase, β-glucuronidase, and uridine 5'-diphosphoglucose (UDPG) were purchased from Sigma-Aldrich (St. Louis, MO). β-Nicotinamide adenine dinucleotide phosphate (NADPH) tetrasodium salt was obtained from Calbiochem (San Diego, CA). Ketoconazole, tranylcypromine, α-naphthoflavone, quinidine, and β-glucuronidase were purchased from MP Biochemicals (Solon, OH). Pooled human liver microsomes were purchased from Puracyp (Carlsbad, CA). Mice and rat liver microsomes were prepared from male C57BL/6 mice and male CD rats, respectively (Chen et al., 2006). The microsomal protein concentration was determined by bicinchoninic acid (BCA) protein assay.

Animal treatment and sample collection. Male C57BL/6 mice (10 to 12-week old) and male CD rats (200-250 g) from Charles River Laboratories (Wilmington, MA) were used in this study (Wiener and Reith, 1990). All animals were maintained in a University of Minnesota (UMN) animal facility under a standard 12 h light/12 h dark cycle with food and water *ad*

libitum. Handling and treatment procedures were in accordance with animal study protocols approved by the UMN Animal Care and Use Committee.

For cocaine treatment, unlabeled cocaine and deuterated cocaine ([$^2H_5$-*phenyl*]-cocaine and [$^2H_3$-*N-methyl*]-cocaine) were dissolved in a saline solution and administered at the dose of 30 mg/kg by intraperitoneal (i.p.) injection. Control animals were treated with blank saline solution. Urine samples were collected by housing animals in the metabolic cages. Liver and other tissue samples were harvested after animals were euthanized by carbon dioxide. All urine and tissue samples were stored at -80°C before further analysis.

Assessment of CIH. General histology of liver samples was examined by hematoxylin and eosin (H & E) staining. Serum alanine aminotransferase (ALT) activity was measuring using an assay kit (Pointe Scientific, Canton, MI). Briefly, 5 μL serum was mixed with 200 μL ALT assay buffer, and the oxidation of NADH to NAD$^+$ was monitored at 340 nm for 5 min.

Liquid chromatography-mass spectrometry (LC-MS) analysis of urine samples. To avoid the loss of cocaine metabolites in sample preparation, minimal sample cleanup was performed prior to LC-MS analysis. Deproteinization of urine samples from mice and rats was conducted by mixing one volume of urine with 5 volumes of 50% aqueous acetonitrile. After a 10-min centrifugation at 14,000 × g, a 5-μL aliquot of diluted urine samples was injected into a Waters Acquity^{TM} ultra-performance liquid chromatography (UPLC) system (Milford, MA) and separated by a gradient of mobile phase ranging from water to 95% aqueous acetonitrile containing 0.1% formic acid over a 10-min run. LC eluate was introduced into a Waters SYNAPT QTOF mass spectrometer (QTOF-MS) for accurate mass measurement and MS/MS analysis. Capillary voltage and cone voltage were maintained at 3.2 kV and 30 V, respectively, in positive electrospray ionization (ESI). Source temperature and desolvation temperature were

7

set at 120°C and 350°C, respectively. Nitrogen was used as both cone gas (50 L/h) and desolvation gas (700 L/h), and argon as the collision gas. For accurate mass measurement, the mass spectrometer was calibrated with sodium formate solution (range *m/z* 50-1000) and monitored by the intermittent injection of the lock mass leucine enkephalin ($[M+H]^+ = 556.2771$ *m/z*) in real time. Mass chromatograms and mass spectral data were acquired and processed by MassLynx software (Waters) in centroid format. Accurate mass value and isotopic peak intensity were used to calculate the elemental composition. Additional structural information was obtained by tandem MS (MS/MS) fragmentation with collision energies ranging from 15 to 40 eV.

Chemometric analysis and cocaine metabolite identification. Chromatographic and spectral data of urine samples were deconvoluted by MarkerLynx™ software (Waters). A multivariate data matrix containing information on sample identity, ion identity (RT and *m/z*) and ion abundance was generated through centroiding, deisotoping, filtering, peak recognition and integration. The intensity of each ion was calculated by normalizing the single ion counts (SIC) *versus* the total ion counts (TIC) in the whole chromatogram. The data matrix was further exported into SIMCA-P+™ software (Umetrics, Kinnelon, NJ), and transformed by mean-centering and *Pareto* scaling, a technique that increases the importance of low abundance ions without significant amplification of noise. Principal components analysis (PCA) was adopted to analyze the urine data from control and cocaine-treated animals. Major latent variables in the data matrix were described in a scores scatter plot of multivariate model. Cocaine metabolites were identified by analyzing ions contributing to the principal components and to the separation of sample groups in the loadings scatter plot. The chemical identities of cocaine metabolites were determined by accurate mass measurement, elemental composition analysis, MS/MS fragmentation, and comparisons with authentic standards if available.

Profiling cocaine metabolism in the mouse and rat. The chromatographic peaks of all identified urinary cocaine metabolites were identified and their peak areas were determined using accurate mass measurement-based MetaboLynx^{TM} software (Waters) (Chen et al., 2007b). The profiles of urinary cocaine metabolites in mouse and rat were compared by calculating the percentage of the peak area of each single metabolite in the pooled total peak area (area % ±SD) of cocaine and all identified metabolites. The same data analysis approach was also applied to profile the phase I metabolites after the incubation of cocaine with liver microsomes.

Liver microsomal incubations. In vitro incubations of cocaine with liver microsomes were carried out at 37°C in a 96-well plate using a Jitterbug incubator (Boekel Scientific). The reaction mix contains cocaine (500 μM), mouse, rat or human liver microsomes (1 mg protein/mL), NADPH (1 mM), MgCl$_2$ (3 mM) in 100 mM phosphate buffer (pH 7.4) in a total volume of 200 µL. After a 30-min incubation, the reactions were terminated by adding an equal volume of acetonitrile, followed by vortexing and centrifugation at 14,000 × g for 10 min. The supernatants were transferred to HPLC vials for LC-MS analysis.

Chemical inhibition of in vitro cocaine metabolism. Known P450 inhibitors, including α-naphthoflavone (ranging from 10 nM to 1 μM), tranylcypromine (ranging from 20 nM to 2 μM), orphenadrine (ranging from 10 µM to 1 mM), sulfaphenazole (ranging from 200 nM to 20 µM), quinidine (ranging from 20 nM to 2 µM), and ketoconazole (ranging from 10 nM to 1 µM), were co-incubated with liver microsomes, cocaine, and NADPH in the reaction buffer for 10 minutes. Samples were processed under the same conditions of microsomal reactions as described above.

*In vitro biosynthesis of N-hydroxybenzoylnorecgoine glucoside (**XXIX**).* A mixture of norcocaine (100 μM), mouse liver microsomes (1 mg/mL), NADPH (1 mM), MgCl$_2$ (3 mM), and 100 mM phosphate buffer (pH 7.4) in a final volume of 200 μL was incubated at 37 ^{o}C for

30 min. After adding a mixture of UDPG (4 mM), Brij58 (0.1 mg/mg protein), and mouse liver

microsomes (1 mg/mL), the reaction was continued for another 60 min. For negative control,

either NADPH or UDPG was removed from the reaction. The reaction was terminated by mixing

with an equal volume of acetonitrile. After vortexing and centrifugation, the supernatant was

dried under N_2 and reconstituted in 50 μL of 20% aqueous acetonitrile. The samples were

analyzed by LC-MS.

Enzymatic hydrolysis of conjugated cocaine metabolites in urine. The glucoside moiety

of metabolite **XXIX** was confirmed by incubating mouse urine samples with α-glucosidase (20

U/mL) and β-glucosidase (20 U/mL) for 4 h, respectively. The glucuronide moiety of

metabolites **XXX-XXXXII** was confirmed by incubating rat urine samples with β-glucuronidase

(8 U/μL) for 1 h. The formation of aglycones after the incubations was determined by LC-MS

analysis.

Statistics. Experimental values are expressed as mean ± standard deviation (SD).

Statistical analysis was performed with two-tailed Student's *t*-tests for unpaired data, with a *p*-

value of <0.05 considered as statistically significant.

Results

Differential response from the mouse and rat to cocaine treatment. To compare their

toxicological responses to cocaine treatment, both C57BL/6 mice and CD rats were treated with

daily i.p. injection of 30 mg/kg cocaine. The mice after a 3-day cocaine treatment were lethargic

and ungroomed, but the rats appeared normal even after a 7-day cocaine exposure. Examination

of serum alanine transferase (ALT) activity revealed dramatic elevation of ALT activity in the

mouse, but not in the rat (**Fig. 1A**). The differential responses from the mouse and rat were

further confirmed by the histological analysis, which showed that extensive necrosis occurred in the centrilobular region of the mouse liver (**Fig. 1B**), but not in the rat liver (data not shown). More details on the phenotypes of CIH in the mouse were reported elsewhere (Shi et al.).

Metabolomic comparisons of urine samples from the mice and rats treated with cocaine. Urine samples from the control and cocaine treatments were examined by the LC-MS-based metabolomics. After processing the data acquired from the LC-MS analysis by principal components analysis (PCA), the multivariate models were constructed to determine the metabolic differences between the control and cocaine treatments. The separation of cocaine-treated samples from corresponding controls was evident in the scores scatter plot of the PCA model on mouse urine (**Fig. 2A**). The loadings scatter plot of the model showed that the compounds highly correlated to the cocaine treatment (encircled in **Fig. 2B**) were mainly cocaine and cocaine metabolites due to their absence in the control urine. Similarly, the rat urine samples were also separated in a PCA model in accordance with the cocaine treatment (**Fig. 2C**), and the separation was also mainly due to cocaine and its metabolites (**Fig. 2D**). Even though both mouse and rat had a similar pattern of separation in the PCA models (**Fig. 2A** and **2C**), further examination of the loadings plots revealed that the compounds contributing to the separation of control and cocaine-treated samples in the mouse model and the rat model were different cocaine metabolites (labeled in **Fig. 2B** and **2D**). Therefore, different cocaine metabolism occurs in the two rodent species.

Profiling cocaine metabolism in the mouse and rat. Comprehensive identifications of urinary cocaine metabolites in the mouse and rat were performed based on their none-or-all distribution pattern in the control and cocaine-treated animals and their contributions to the separation of the cocaine-treated animals from the controls in the PCA model (**Fig. 2**).

11

Confirmation of urinary ions as cocaine metabolites was achieved through the comparative analysis of urine samples from the treatments of two deuterated cocaine isotopomers, [$^2H_3$-*N-methyl*]-cocaine and [$^2H_5$-*phenyl*]-cocaine (data not shown). The structures of identified cocaine metabolites were defined through a combination of accurate mass measurement, elemental composition analysis, tandem MS analysis (MS/MS), chromatographic and spectroscopic comparison with available authentic standards (**Fig. 3** and **Supplemental Fig. 1A-W**). In total, cocaine and its 41 urinary cocaine metabolites were identified from this analytical process (**Fig. 3**). Among them, the metabolite **XXIX** and a series of glucuronides (**XXX-XXXXII**) have not been reported previously (the details of structural elucidation are described below). Based on the structures of identified cocaine metabolites, this metabolomics-based metabolite analysis was capable of identifying both major and minor cocaine metabolites formed by diverse phase I reactions, including hydrolysis, dealkylation, hydroxylation, and *N*-oxidation, and phase II conjugation reactions, including methylation, glucuronidation, and glucosidation. The profile of cocaine metabolism in the mouse and rat was further determined by calculating the relative peak area of individual metabolites in the total peak area of all identified cocaine metabolites. The results revealed that cocaine metabolism differed dramatically between the mouse and rat (**Table 1**): *1)*. more cocaine remained unmetabolized in the mouse urine than the rat urine. *2)*. the level of benzoylecgonine (**V**), a major cocaine metabolite from the ester hydrolysis, was comparable between the two species. *3)*. the levels of metabolites **II**, **IV**, **VI**, **VIII**, and **XXIX** originated from *N*-demethylation and *N*-hydroxylation, two known bioactivation reactions, were much higher in the mouse than their levels in the rat, while the relative abundances of metabolites **IX-XI**, **XIII-XVI**, **XIX-XXVIII**, and **XXX-XXXXII** formed by aryl hydroxylation and subsequent phase II conjugations were much higher in the rat than their levels in the mouse. Therefore, the

metabolic reactions in the ecgonine moiety of cocaine were more dominant in the mouse, while the metabolic reactions in the benzoyl moiety of cocaine were far more common in the rat. One notable observation is that the level of cocaine *N*-oxide (**XII**) did not differ between the mouse and rat urine (**Table 1**), indicating that FMO-mediated cocaine metabolism was comparable in two species. In addition, *N*-hydroxynorcocaine (NHNC), an important intermediate metabolite in cocaine bioactivation, was not observed in the urine even though its downstream metabolite, *N*-hydroxybenzoylecgonine (**VIII**) was detected. It is possible, due to its high reactivity, NHNC was rapidly converted to other species before urinary excretion (Misra et al., 1979; Lloyd et al., 1993).

Characterization of novel cocaine metabolites in the mouse and rat. A novel glucoside conjugate (**XXIX**, exact mass: [M+H]$^+$=454.1713 *m/z*) of *N*-hydroxybenzoylnorecgonine (**VIII**) in the mouse was characterized based on evidence from multiple sources. *1).* The metabolite was determined as a product of *N*-demethylation reaction since the same protonated ion ([M+H]$^+$=454.1718 *m/z*) was also detected in the urine samples from the mice treated with [$^2H_3$-*N-methyl*]-cocaine, indicating that the methyl group containing 3 deuterium atoms in [$^2H_3$-*N-methyl*]-cocaine was removed during the formation of metabolite **XXIX**. This conclusion was further supported by the *in vitro* biosynthesis of metabolite **XXIX** from norcocaine (**VI**), which is *N*-demethylated cocaine (data not shown). *2).* Besides *N*-demethylation, additional structural modifications to form metabolite **XXIX** also occurred in the ecgonine moiety of cocaine since none of five deuterium atoms in the benzoyl moiety of [$^2H_5$-*phenyl*]-cocaine were removed in the formation of deuterated metabolite **XXIX** ([M+H]$^+$=459.2012 *m/z*). *3).* Neutral loss of 162 from the parent ion (454 *m/z*) to the daughter ion (292 *m/z*) in the MS/MS fragmentation analysis (**Fig. 4A**) indicated the existence of a glucose moiety, which was confirmed by the abovementioned

13

biosynthesis reaction using norcocaine, mouse liver microsomes, and UDP-glucose. In addition, the glucose moiety can be removed by the treatment of α-glucosidase, but not by β-glucosidase, suggesting the glucoside is in the α-configuration. *4*). *N*-hydroxybenzoylnorecgonine as the aglycone was confirmed by comparing the fragmentation pattern of metabolite **XXIX** with that of *N*-hydroxybenzoylnorecgonine (**VIII**) (**Fig. 4A** and **Supplemental Fig. 1H**).

A similar analytical approach was applied to define a group of 29 arylhydroxy and arylhydroxymethoxy metabolites (**XIII-XXVIII** and **XXX-XXXXII**) in the rat. Among them, dual substitutions on the phenyl ring by hydroxyl and methoxy functional groups have been reported previously (Smith, 1984; Smith et al., 1984). However, the metabolites (**XXI**-**XXIII**, **XXVII**, **XXVIII**, **XXXV**-**XXXVIII**, **XXXXI**, and **XXXXII**) formed by triple substitutions with hydroxy and methoxy function groups are novel metabolites. For example, metabolites **XXXXI** and **XXXXII** (exact mass: $[M+H]^+$=556.2030 *m/z*), the two abundant hydroxydimethoxycocaine glucuronides in the rat urine, were not formed through the *N*-demethylation reaction since the methyl group containing 3 deuterium atoms in $[^2H_3$-*N-methyl*]-cocaine was not removed during the biosynthesis of deuterated metabolites **XXXXI** and **XXXXII** ($[M+H]^+$=559.2311 *m/z*). Triple substitutions in their structures were identified based on the disappearance of three deuterium atoms in the benzoyl moiety of deuterated metabolites **XXXXI** and **XXXXII** ($[M+H]^+$=558.2152 *m/z*) after the treatment of $[^2H_5$-*phenyl*]-cocaine, while the glucuronosyl moiety were determined through observing the neutral loss of 176 from the parent ion (556 *m/z*) to the daughter ion (380 *m/z*) in the MS/MS fragmentation (**Fig. 4B**) and the detection of aglycone after the *in vitro* β-glucuronidase incubation (data not shown).

In vitro phase I cocaine metabolism catalyzed by mouse, rat and human liver microsomes. To confirm the observed species-dependent differences in *in vivo* cocaine metabolism, the

incubations of cocaine with mouse, rat, and human liver microsomes (MLM, RLM, and HLM) were performed. The formation of phase I metabolites (**II-XIV**) through hydrolysis, *N*-demethylation, *N*-hydroxylation, aryl hydroxylation reactions *in vitro* were examined (**Fig. 5A-C**), and the relative abundances of individual metabolites in the total pool of phase I metabolites were compared (**Fig. 5D**). The results showed that the majority of phase I metabolites in urine were also detected after the microsomal incubation. In addition, *N*-hydroxynorcocaine (NHNC) was present after the microsomal incubation even though it was absent in urine (**Fig. 5A-C** and **Supplemental Fig. 1X**). The distribution of norcocaine (**VI**) and NHNC confirmed that *N*-oxidation reactions were more preferred in the mouse than in the rat, while the distribution of hydroxycocaine (**XI**) and dihydroxycocaine (**XIII** and **XIV**) clearly indicated that aryl hydroxylation reactions occurred as major metabolic events in the rat, but as minor events in the mouse and human (**Fig. 5D**). Overall, the results of microsomal incubations were largely consistent with the observed species-dependent differences in the urinary profiling (**Table 1**).

Potential roles of P450s in species-dependent cocaine metabolism. The contribution of P450 enzymes on differential cocaine metabolism in MLM and RLM was further examined by the co-incubation of cocaine with a panel of direct P450 inhibitors, including α-naphthoflavone (CYP1A inhibitor), tranylcypromine (CYP2A inhibitor), orphenadrine (CYP2B inhibitor), sulfaphenazole (CYP2C inhibitor), quinidine (CYP2D inhibitor), and ketoconazole (CYP3A inhibitor). Within the tested dose ranges, orphenadrine was the only inhibitor that was capable of inhibiting all examined oxidative reactions of cocaine catalyzed by MLM and RLM (**Fig. 6A-F**). Ketoconazole was almost equally effective as orphenadrine in inhibiting the formation of norcocaine (**VI**) and NHNC in MLM (**Fig. 6A-B**), but had little effects on all examined oxidative reactions in RLM (**Fig. 6C-F**). Besides orphenadrine and ketoconazole, other P450 inhibitors

15

had minor or no effect on cocaine metabolism *in vitro*. Therefore, the results from this inhibition assay suggested that the oxidative metabolism of cocaine might be dominated by the CYP2B-catalyzed reactions in the rat, but contributed by both CYP2Bs and CYP3As in the mouse.

Discussion

Cocaine metabolism has been investigated extensively with rodent models and *in vitro* reaction systems (Shuster, 1992). The potential role of cocaine metabolism in the susceptibility to CIH in the mouse and rat has been proposed (Roberts et al., 1992), but experimental evidence that directly supports this correlation was largely absent. In this study, dramatic differences between two rodent species in cocaine metabolism were revealed through metabolomics-based comparisons of their urinary cocaine metabolites (**Table 1**). The most significant differences are the preferred sites of oxidative metabolism in the mouse and rat, as indicated by the facts that the mouse had much higher levels of urinary metabolites from *N*-demethylation and *N*-hydroxylation in the ecognine moiety while the rat had much higher levels of urinary metabolites from aryl hydroxylation in the benzoic acid moiety. The dominance of aryl hydroxylation in the rat was demonstrated by detecting over 30 aryl hydroxy cocaine metabolites in urine, in which the most abundant ones (**XXXXI-XXXXII**) were formed through three aryl hydroxylation reactions. Because *N*-oxidation reactions are mainly responsible for the metabolic activation of cocaine while aryl hydroxylation reactions facilitate the excretion of cocaine, the extensive aryl hydroxylation could be considered as a protective mechanism to reduce the formation of reactive cocaine metabolites in the rat. It should be noted that the formations of aryl hydroxy cocaine metabolites in mouse, rat, and human have been observed previously (Jindal and Lutz, 1986; Zhang and Foltz, 1990; Watanabe et al., 1993). However, the protective functions of aryl

hydroxylation against CIH was not implicated in those studies since these metabolites were assumed as the minor metabolites of cocaine and therefore were not thought to have major roles in affecting the toxicity of cocaine. In this study, the metabolite profiling revealed that aryl hydroxy metabolites are actually major metabolites in the rat despite being minor metabolites in the mouse (**Table 1** and **Fig. 3**). Consistent with this observation *in vivo*, the microsomal incubations also showed that rat liver was much more capable of synthesizing aryl hydroxy metabolites *in vitro* than its mouse counterpart (**Fig. 5A-B**). All together, the association between cocaine metabolism and the susceptibility to the CIH in this study suggested that a competition between aryl hydroxylation and *N*-oxidation reactions in the rat reduces the risk of cocaine exposure to the liver. Another interesting observation regarding the oxidative metabolism was that due to the lack of the aryl hydroxylation activity, phase I cocaine metabolism by HLM resembles MLM more than RLM, suggesting that *N*-oxidation reactions are likely to be the dominant metabolic route in humans. Therefore, the mouse could be a more appropriate experimental animal model than the rat for examining the toxic and pathophysiological effects associated with *N*-oxidized cocaine metabolites.

Enzymes responsible for the *N*-oxidation reactions have been extensively investigated in previous studies, but the enzymes responsible for the aryl hydroxylation have not been examined in detail. The involvement of several P450 enzymes, including CYP1A, CYP2A, CYP2B, and CYP3A, and FMOs in the metabolic activation of cocaine through the *N*-demethylation and *N*-hydroxylation reactions has been demonstrated or implicated in those studies, and the relative importance of individual enzymes in cocaine metabolism appeared to be reaction-dependent, as well as species-, strain-, and sex-dependent (Kloss et al., 1982; Boelsterli et al., 1992; Pellinen et al., 1994; Aoki et al., 2000; Pellinen et al., 2000). Since the similar abundances of cocaine *N*-

oxide (**XII**), the direct product of FMO-mediated oxidation, were observed in the metabolite profiling of mouse and rat urine in this study (**Table 1**), P450-mediated reactions, instead of FMO-mediated reaction, are likely the major contributor to differential phase I cocaine metabolism in the mouse and rat. The results from the chemical inhibition assay in this study showed that the inhibitors of CYP2B and CYP3A enzymes were much more effective than the inhibitors of other P450s (**Fig. 6**). The observation of strong inhibitory effects of orphenadrine against the *N*-oxidation and aryl hydroxylation in the RLM indicated that CYP2B enzymes are probably the dominant catalysts in the oxidative metabolism of cocaine in the rat, while the observation of comparable inhibitory effects of ketoconazole and orphenadrine against the *N*-oxidation in the MLM suggested that both CYP2B and CYP3A could contribute to the biotransformation of cocaine in the mouse (**Fig. 6**). It is interesting that even though CYP2B enzymes are involved in cocaine metabolism in both rodent species, especially the rat, the metabolic consequences of these activities were different, as evidenced by the lack of aryl hydroxylation in the mouse and the domination of aryl hydroxylation in the rat. It is possible that the genetic variances, protein expression and enzymatic properties of CYP2B isoforms in the mouse and rat contribute to these differences (Lewis and Lake, 1997; Martignoni et al., 2006). However, how these variances affect the species-, strain-, or sex-dependent cocaine metabolism is not fully resolved and will require further examinations.

Novel cocaine metabolites from glucuronidation and glucosidation reactions were identified in this study. Even though unreported before, the existence of the glucuronide conjugates of aryl hydroxy cocaine and norcocaine (**XXX**-**XXXXII**) in the rat was not unexpected, since glucuronidation is a common reaction for phenolic compounds. However, the detection of the glucoside conjugate of *N*-hydroxybenzoylnorcocaine (**XXIX**), instead of its

18

glucuronide conjugate, in the mouse was unexpected and revealed a novel metabolic route in cocaine metabolism. Glucosidation, especially in the α-configuration, is a rather uncommon conjugation reaction occurring to exogenous chemicals in mammals (Kamimura et al., 1988; Tang, 1990). Based on the general functions of conjugation reactions, the formation of *N*-hydroxybenzoylnorcocaine glucoside (**XXIX**) is likely a metabolic event that facilitates the excretion of *N*-oxidation cocaine metabolites. It is noteworthy that the appearance of this glucoside was associated with a high abundance of its aglycone, *N*-hydroxybenzoylnorcocaine (**VIII**), in mouse urine, which suggests that certain structural properties of *N*-hydroxybenzoylnorcocaine make it a preferred substrate for glucosidation rather than glucuronidation. Although a NMR analysis has not been conducted to resolve the site of glucosidation due to the difficulty in obtaining sufficient pure compound from the biosynthetic reaction conducted in this study, additional structural information was obtained through the MS/MS fragmentation and glucosidase treatment, which revealed that the glucosidation occurs in the ecgonine moiety of cocaine and the glucoside is likely in the α-configuration through the O-glucosidation reaction (**Fig. 4A**). Because the glucoside metabolite was only detected in the CIH-susceptible mouse but absent in the CIH-resistant rat, further studies on its distribution, especially in the human urine after cocaine overdose, and its correlation with CIH, will define its potential value as a biomarker of CIH.

Compared to previous studies on cocaine metabolism in the mouse and rat, the metabolomics-guided metabolite profiling in this study provides the first comprehensive comparisons of *in vivo* cocaine metabolism in the mouse and rat. Metabolomics is very efficient in identifying novel xenobiotic metabolites and defining the pattern of xenobiotic metabolism, especially when multiple metabolic routes exist in the body (Johnson et al.; Chen et al., 2007a).

DMD #48678

Besides its value as a tool for probing xenobiotic metabolism, metabolomics is also very capable for examining changes in endogenous metabolism induced by chemical treatment, genetic modification, and health status (Nicholson and Wilson, 2003; Idle and Gonzalez, 2007). In a separate study on the causes of CIH in the mouse, metabolomic and lipidomic analyses have led to the identification of cocaine-induced inhibition of fatty acid oxidation and the time-dependent increase of cocaine bioactivation during a 3-day subacute cocaine treatment (Shi et al.).

Overall, a combination of metabolite profiling of cocaine metabolism *in vivo* and *in vitro*, together with stable isotope tracing and chemical inhibition in this study led to the identification of novel cocaine metabolites, and revealed differential cocaine metabolism in the mouse and rat, which is likely due to the different catalytic activities of P450s (CYP2B and CYP3A). The high *N*-oxidation activities in the mouse may explain its susceptibility to CIH while the high aryl hydroxylation activities in the rat contribute to its resistance to CIH.

DMD #48678

Authorship Contributions

Participated in research design: Chen and Gosnell.

Conducted experiments: Yao, Shi, and Wang.

Performed data analysis: Yao, Chen, and Shi.

Wrote or contributed to the writing of the manuscript: Chen, Yao, Gosnell, Shi, and Wang.

References

Aoki K, Takimoto M, Ota H and Yoshida T (2000) Participation of CYP2A in cocaine-induced hepatotoxicity in female mice. *Pharmacol Toxicol* **87:**26-32.

Boelsterli UA and Goldlin C (1991) Biomechanisms of cocaine-induced hepatocyte injury mediated by the formation of reactive metabolites. *Arch Toxicol* **65:**351-360.

Boelsterli UA, Lanzotti A, Goldlin C and Oertle M (1992) Identification of cytochrome P-450IIB1 as a cocaine-bioactivating isoform in rat hepatic microsomes and in cultured rat hepatocytes. *Drug Metab Dispos* **20:**96-101.

Boyer CS, Ross D and Petersen DR (1988) Sex and strain differences in the hepatotoxic response to acute cocaine administration in the mouse. *J Biochem Toxicol* **3:**295-307.

Chen C, Gonzalez FJ and Idle JR (2007a) LC-MS-based metabolomics in drug metabolism. *Drug Metab Rev* **39:**581-597.

Chen C, Ma X, Malfatti MA, Krausz KW, Kimura S, Felton JS, Idle JR and Gonzalez FJ (2007b) A comprehensive investigation of 2-amino-1-methyl-6-phenylimidazo[4,5-b]pyridine (PhIP) metabolism in the mouse using a multivariate data analysis approach. *Chem Res Toxicol* **20:**531-542.

Chen C, Meng L, Ma X, Krausz KW, Pommier Y, Idle JR and Gonzalez FJ (2006) Urinary metabolite profiling reveals CYP1A2-mediated metabolism of NSC686288 (aminoflavone). *J Pharmacol Exp Ther* **318:**1330-1342.

Evans MA (1983) Role of protein binding in cocaine-induced hepatic necrosis. *J Pharmacol Exp Ther* **224:**73-79.

Evans MA and Harbison RD (1978) Cocaine-induced hepatotoxicity in mice. *Toxicol Appl Pharmacol* **45:**739-754.

Gottfried MR, Kloss MW, Graham D, Rauckman EJ and Rosen GM (1986) Ultrastructure of experimental cocaine hepatotoxicity. *Hepatology* **6:**299-304.

Idle JR and Gonzalez FJ (2007) Metabolomics. *Cell Metab* **6:**348-351.

Jindal SP and Lutz T (1986) Ion cluster techniques in drug metabolism: use of a mixture of labeled and unlabeled cocaine to facilitate metabolite identification. *J Anal Toxicol* **10:**150-155.

Johnson CH, Patterson AD, Idle JR and Gonzalez FJ Xenobiotic metabolomics: major impact on the metabolome. *Annu Rev Pharmacol Toxicol* **52:**37-56.

Kamimura H, Kawai R and Kudo H (1988) Metabolic fate of indeloxazine hydrochloride: alpha-glucoside formation in rats. *Xenobiotica* **18:**141-149.

Kanel GC, Cassidy W, Shuster L and Reynolds TB (1990) Cocaine-induced liver cell injury: comparison of morphological features in man and in experimental models. *Hepatology* **11:**646-651.

Kloss MW, Cavagnaro J, Rosen GM and Rauckman EJ (1982) Involvement of FAD-containing monooxygenase in cocaine-induced hepatotoxicity. *Toxicol Appl Pharmacol* **64:**88-93.

Kloss MW, Rosen GM and Rauckman EJ (1983) N-demethylation of cocaine to norcocaine. Evidence for participation by cytochrome P-450 and FAD-containing monooxygenase. *Mol Pharmacol* **23:**482-485.

Kloss MW, Rosen GM and Rauckman EJ (1984) Cocaine-mediated hepatotoxicity. A critical review. *Biochem Pharmacol* **33:**169-173.

Knuepfer MM (2003) Cardiovascular disorders associated with cocaine use: myths and truths. *Pharmacol Ther* **97:**181-222.

Lakoski JM, Galloway MP and White FJ (1992) *Cocaine : pharmacology, physiology, and clinical strategies*. CRC Press, Boca Raton.

Lason W (2001) Neurochemical and pharmacological aspects of cocaine-induced seizures. *Pol J Pharmacol* **53:**57-60.

Lewis DF and Lake BG (1997) Molecular modelling of mammalian CYP2B isoforms and their interaction with substrates, inhibitors and redox partners. *Xenobiotica* **27:**443-478.

Lloyd RV, Shuster L and Mason RP (1993) Reexamination of the microsomal transformation of N-hydroxynorcocaine to norcocaine nitroxide. *Mol Pharmacol* **43:**645-648.

Marks V and Chapple PA (1967) Hepatic dysfunction in heroin and cocaine users. *Br J Addict Alcohol Other Drugs* **62:**189-195.

Martignoni M, Groothuis GM and de Kanter R (2006) Species differences between mouse, rat, dog, monkey and human CYP-mediated drug metabolism, inhibition and induction. *Expert Opin Drug Metab Toxicol* **2:**875-894.

Masini A, Gallesi D, Giovannini F, Trenti T and Ceccarelli D (1997) Membrane potential of hepatic mitochondria after acute cocaine administration in rats--the role of mitochondrial reduced glutathione. *Hepatology* **25:**385-390.

Mehanny SZ and Abdel-Rahman MS (1991) Cocaine hepatotoxicity in mice: histologic and enzymatic studies. *Toxicol Pathol* **19:**24-29.

Misra AL, Pontani RB and Vadlamani NL (1979) Metabolism of norcocaine, N-hydroxy norcocaine and cocaine-N-oxide in the rat. *Xenobiotica* **9:**189-199.

Ndikum-Moffor FM, Schoeb TR and Roberts SM (1998) Liver toxicity from norcocaine nitroxide, an N-oxidative metabolite of cocaine. *J Pharmacol Exp Ther* **284:**413-419.

Nicholson JK, Connelly J, Lindon JC and Holmes E (2002) Metabonomics: a platform for studying drug toxicity and gene function. *Nat Rev Drug Discov* **1:**153-161.

Nicholson JK and Wilson ID (2003) Opinion: understanding 'global' systems biology: metabonomics and the continuum of metabolism. *Nat Rev Drug Discov* **2:**668-676.

Nutt D, King LA, Saulsbury W and Blakemore C (2007) Development of a rational scale to assess the harm of drugs of potential misuse. *Lancet* **369:**1047-1053.

Patkar AA, Rozen S, Mannelli P, Matson W, Pae CU, Krishnan KR and Kaddurah-Daouk R (2009) Alterations in tryptophan and purine metabolism in cocaine addiction: a metabolomic study. *Psychopharmacology (Berl)* **206:**479-489.

Pellinen P, Honkakoski P, Stenback F, Niemitz M, Alhava E, Pelkonen O, Lang MA and Pasanen M (1994) Cocaine N-demethylation and the metabolism-related hepatotoxicity can be prevented by cytochrome P450 3A inhibitors. *Eur J Pharmacol* **270:**35-43.

Pellinen P, Kulmala L, Konttila J, Auriola S, Pasanen M and Juvonen R (2000) Kinetic characteristics of norcocaine N-hydroxylation in mouse and human liver microsomes: involvement of CYP enzymes. *Arch Toxicol* **74:**511-520.

Perino LE, Warren GH and Levine JS (1987) Cocaine-induced hepatotoxicity in humans. *Gastroenterology* **93:**176-180.

Powers JF, Alroy J and Shuster L (1992) Hepatic morphologic and biochemical changes induced by subacute cocaine administration in mice. *Toxicol Pathol* **20:**61-70.

Roberts SM, James RC and Harbison RD (1992) *Cocaine-induced hepatotoxicity (Chapter 2 of Cocaine: pharmacology, physiology, and clinical strategies)*. CRC Press, Boca Raton.

Shi X, Yao D, Gosnell BA and Chen C Lipidomic profiling reveals protective function of fatty acid oxidation in cocaine-induced hepatotoxicity. *J Lipid Res*.

DMD #48678

Shuster L (1992) *Pharmacokinetics, metabolism, and disoposition of cocaine (Chapter 1 of Cocaine: pharmacology, physiology, and clinical strategies).* CRC Press, Boca Raton.

Shuster L, Casey E and Welankiwar SS (1983) Metabolism of cocaine and norcocaine to N-hydroxynorcocaine. *Biochem Pharmacol* **32:**3045-3051.

Shuster L, Garhart CA, Powers J, Grunfeld Y and Kanel G (1988) Hepatotoxicity of cocaine. *NIDA Res Monogr* **88:**250-275.

Smith RM (1984) Arylhydroxy metabolites of cocaine in the urine of cocaine users. *J Anal Toxicol* **8:**35-37.

Smith RM, Poquette MA and Smith PJ (1984) Hydroxymethoxybenzoylmethylecgonines: new metabolites of cocaine from human urine. *J Anal Toxicol* **8:**29-34.

Tang BK (1990) Drug glucosidation. *Pharmacol Ther* **46:**53-56.

Thompson ML, Shuster L, Casey E and Kanel GC (1984) Sex and strain differences in response to cocaine. *Biochem Pharmacol* **33:**1299-1307.

Thompson ML, Shuster L and Shaw K (1979) Cocaine-induced hepatic necrosis in mice--the role of cocaine metabolism. *Biochem Pharmacol* **28:**2389-2395.

Toennes SW, Thiel M, Walther M and Kauert GF (2003) Studies on metabolic pathways of cocaine and its metabolites using microsome preparations from rat organs. *Chem Res Toxicol* **16:**375-381.

Wanless IR, Dore S, Gopinath N, Tan J, Cameron R, Heathcote EJ, Blendis LM and Levy G (1990) Histopathology of cocaine hepatotoxicity. Report of four patients. *Gastroenterology* **98:**497-501.

Watanabe K, Hida Y, Matsunaga T, Yamamoto I and Yoshimura H (1993) Formation of p-hydroxycocaine from cocaine by hepatic microsomes of animals and its pharmacological effects in mice. *Biol Pharm Bull* **16:**1041-1043.

Wiener HL and Reith ME (1990) Differential effects of daily administration of cocaine on hepatic and cerebral glutathione in mice. *Biochem Pharmacol* **40:**1763-1768.

Zhang JY and Foltz RL (1990) Cocaine metabolism in man: identification of four previously unreported cocaine metabolites in human urine. *J Anal Toxicol* **14:**201-205.

DMD #48678

Footnotes

Reprint requests should be addressed to the corresponding author Dr. Chi Chen, Department of

Food Science and Nutrition, University of Minnesota, 1334 Eckles Avenue, 225 FScN, St. Paul,

MN 55108, Tel.: 612-624-7704; Fax: 612-625-5272; Email: chichen@umn.edu

26

DMD #48678

Figure legends

Fig. 1. Different susceptibility to cocaine treatment in the mouse and rat. ***A.*** Serum ALT activity.

B. H & E staining of control and cocaine-treated mouse liver ($100 \times$ magnification). ** ($p<0.01$)

indicates statistical significance between control and cocaine treatment.

Fig. 2. Metabolomic analysis of urine samples from the control and cocaine-treated mice and

rats. Data acquisition and analysis are described in the *Materials and Methods*. ***A.*** Scores scatter

plot of the PCA model on urine samples from the control (Δ) and cocaine-treated ($\blacktriangle$) mice (n=4).

The t[1] and t[2] values represent the scores of each sample in principal component 1 and 2,

respectively. ***B.*** Loadings scatter plot of all detected ions from mouse urine in the PCA model.

The p[1] and p[2] values represent the contributing weights of each ion to principal component 1

and 2. ***C.*** Scores scatter plot of the PCA model on urine samples from the control ($\Diamond$) and

cocaine-treated ($\blacklozenge$) rats (n=6). ***D.*** Loadings scatter plot of all detected ions from rat urine in the

PCA model. Major urinary cocaine metabolites are labeled in two loadings plots. The chemical

identities of these metabolites are presented in the Table 1.

Fig. 3. Metabolic routes of forming 41 cocaine metabolites (**II**-**XXXXII**) identified by

metabolomics-based metabolite profiling. Reactions responsible for generating these metabolites

from cocaine (**I**) include non-enzymatic hydrolysis, esteratic hydrolysis, *N*-demethylation, *N*-

hydroxylation, *N*-oxidation, aryl hydroxylation, *O*-methylation, glucuronidation, and

glucosidation. The solid arrow represents the reaction that is preferred in the mouse. The dashed

arrow represents the reaction that is preferred in the rat. A combination of solid and dashed

arrows represents the reaction that is comparable between the mouse and rat.

27

Fig. 4. Structural elucidation of novel cocaine metabolites. *A.* Representative MS/MS spectrum of *N*-hydroxybenzoylnorecgonine glucoside (**XXIX**) in mouse urine. *B.* Representative MS/MS spectrum of hydroxydimethoxycocaine glucuronides (**XXXXI** and **XXXXII**). Major fragment ions were interpreted in the inlaid structural diagrams.

Fig. 5. *In vitro* metabolism of cocaine by pooled human, mouse and rat liver microsomes. *A-C.* Representative chromatogram of major phase I cocaine metabolites formed by MLM, RLM, and HLM, respectively. Ions within the 20 ppm range of theoretical accurate mass ($[M+H]^+$) of cocaine (**I**) and its metabolites (200.1287, 290.1392, 306.1341, 320.1498, and 336.1447 *m/z*) were extracted and labeled in the chromatograms. The ion intensity of the most abundant metabolites was set arbitrarily as 100%. Major phase I metabolites are labeled. The chemical identities of these metabolites are presented in the Table 1. One unknown metabolite is labeled as "UK". *D.* A comparison of phase I cocaine metabolites formed by microsomal incubations (n=3). Relative abundance of individual cocaine metabolite formed by MLM, RLM, and HLM was represented as a relative peak area (area % $\pm$ SD) by calculating its percentage in the total peak area of all detected phase I cocaine metabolites.

Fig. 6. Effects of P450 inhibitors on microsomal oxidation of cocaine. Incubations of P450 inhibitors, including α-naphthoflavone (α-NF, 0.01-1 μM), tranylcypromine (0.02-2 μM), orphenadrine (0.01-1 mM), sulfaphenazole (0.2-20 μM), quinidine (0.02-2 μM), and ketoconazole (0.01-1 μM), were conducted as described in the *Materials and Methods* (n=3). Inhibitor concentration in the x-axis is expressed as the fold of the highest concentration of

specific inhibitor. The yield of cocaine metabolites from the microsomal incubation without the inhibitor is arbitrarily as 100%. **A.** Effects of P450 inhibitors on the production of norcocaine (**VI**) by MLM. **B**. Effects of P450 inhibitors on the production of *N*-hydroxynorcocaine by MLM. **C.** Effects of P450 inhibitors on the production of norcocaine (**VI**) by RLM. **D.** Effects of P450 inhibitors on the production of *N*-hydroxynorcocaine by RLM. **E**. Effects of P450 inhibitors on the production of hydroxycocaine (**XI**) by RLM. **F**. Effects of P450 inhibitors on the production of dihydroxycocaine (**XIV**) by RLM.
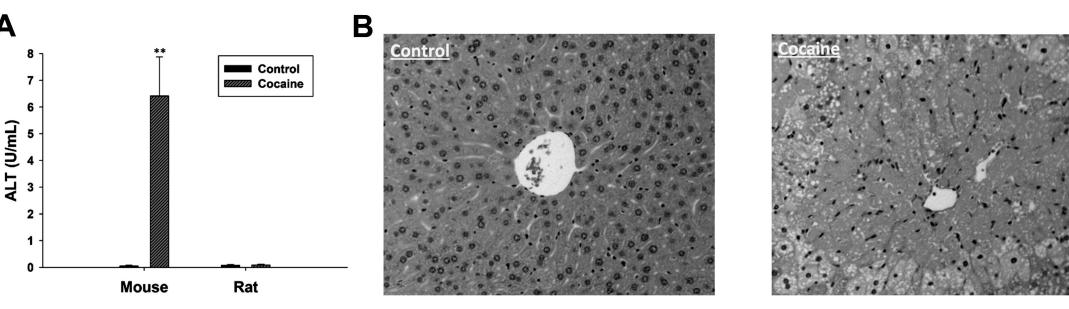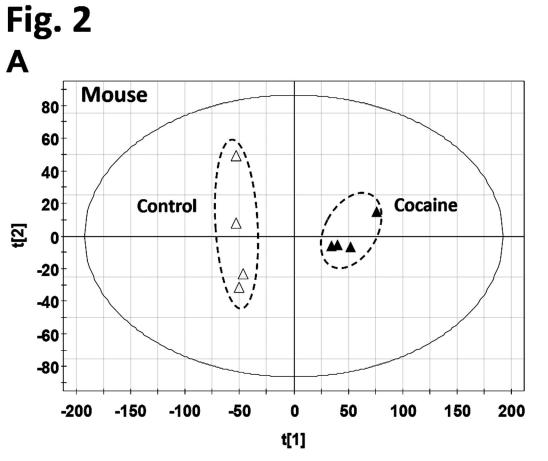
DMD #48678

Table 1. Profiles of urinary cocaine metabolites in the rat and mouse. After i.p. injection of 30 mg/kg cocaine to cocaine-naïve mice and rats, 24-h urine samples were collected. Identification and structural elucidation of cocaine metabolites (**II**-**XXXXII**) through LC-MS and metabolomic analysis were described in the *Materials and Methods*. After integrating the chromatographic peaks of cocaine metabolites using MetaboLynx^{TM} software, the relative signal intensity of each metabolite was represented as a relative peak area (area % $\pm$ SD) by calculating its percentage in the total peak area of cocaine and its urinary metabolites. * ($p<0.05$) and ** ($p<0.01$) indicate that the level of cocaine metabolite in the mouse is statistically higher than that in the rat, while # ($p<0.05$) and ## ($p<0.01$) indicate that the level of cocaine metabolite in the rat is statistically higher than that in the mouse.
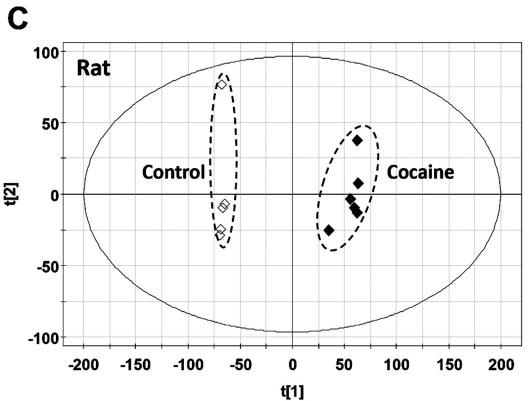
30

ID	Metabolites	Formula	$[M+H]^+$	RT (min)	Rat (Area %)	Mouse (Area %)
I	Cocaine	$C_{17}H_{21}NO_4$	304.1549	3.84	12.01±5.49	26.58±3.26[**]
II	Norecgonine methyl ester	$C_9H_{15}NO_3$	186.1130	0.34	0.24±0.06	0.58±0.07[**]
III	Ecgonine methyl ester	$C_{10}H_{17}NO_3$	200.1287	0.34	2.17±0.35	2.91±0.25[*]
IV	Benzoylnorecgonine	$C_{15}H_{17}NO_4$	276.1236	3.17	0.69±0.42	8.16±0.57[**]
V	Benzoylecgonine	$C_{16}H_{19}NO_4$	290.1392	3.09	39.01±6.4	44.60±2.48
VI	Norcocaine	$C_{16}H_{19}NO_4$	290.1392	4.02	0.14±0.5	1.31±0.2[**]
VII	Hydroxybenzoylnorecgonine	$C_{15}H_{17}NO_5$	292.1185	2.48	0.14±0.22	0.08±0.10
VIII	*N*-hydorxybenzoylnorecgonine	$C_{15}H_{17}NO_5$	292.1185	3.74	0.48±0.53	9.98±1.30[**]
IX	Hydroxybenzoylecgonine	$C_{16}H_{19}NO_5$	306.1341	2.49	7.63±1.46[##]	0.43±0.05
X	Hydroxynorcocaine	$C_{16}H_{19}NO_5$	306.1341	2.88	0.55±0.26[##]	0.04±0.07
XI	Hydroxycocaine	$C_{17}H_{21}NO_5$	320.1498	2.76	1.02±0.31[#]	0.50±0.02
XII	Cocaine-*N*-oxide	$C_{17}H_{21}NO_5$	320.1498	4.16	0.90±0.43	0.93±0.23
XIII-XIV	Dihydroxycocaine	$C_{17}H_{21}NO_6$	336.1447	2.1, 2.34	1.57±0.95[##]	0.01±0.01
XV-XVI	Hydroxymethoxybenzoylecgonine	$C_{17}H_{21}NO_6$	336.1447	2.61, 2.8	1.08±0.34[##]	0.04±0.04
XVII-XVIII	Hydroxymethoxynorcocaine	$C_{17}H_{21}NO_6$	336.1447	3.05, 3.16	0.31±0.25	0.29±0.09
XIX-XX	Hydroxymethoxycocaine	$C_{18}H_{23}NO_6$	350.1604	2.94, 3.04	2.99±0.78[##]	0.33±0.22
XXI-XXIII	Dihydroxymethoxycocaine	$C_{18}H_{23}NO_7$	366.1553	2.39, 2.5, 2.99	1.23±0.60[##]	0.07±0.05
XXIV-XXVI	Hydroxydimethoxynorcocaine	$C_{18}H_{23}NO_7$	366.1553	2.88, 3.21, 3.46	0.86±0.30[##]	ND
XXVII-XXVIII	Hydroxydimethoxycocaine	$C_{19}H_{25}NO_7$	380.1709	3.03, 3.37	3.29±1.23[##]	0.09±0.02
XXIX	*N*-hydroxybenzoylnorecgonine glucoside	$C_{21}H_{27}NO_{10}$	454.1713	4.61	ND	1.50±0.15[**]
XXX-XXXII	Hydroxymethoxynorcocaine glucuronide	$C_{23}H_{29}NO_{12}$	512.1768	2.2, 2.37, 2.61	1.56±0.58[##]	0.22±0.06
XXXIII-XXXIV	Hydroxymethoxycocaine glucuronide	$C_{24}H_{31}NO_{12}$	526.1925	2.12, 2.54	4.10±0.94[##]	0.27±0.04
XXXV-XXXVIII	Dihydroxymethoxycocaine glucuronide	$C_{24}H_{31}NO_{13}$	542.1874	1.93, 2.21, 2.26, 2.36	2.65±0.64[##]	0.09±0.01
XXXIX-XXXX	Hydroxydimethoxynorcocaine glucuronide	$C_{24}H_{31}NO_{13}$	542.1874	2.63, 2.88	1.68±0.58[##]	ND
XXXXI-XXXXII	Hydroxydimethoxycocaine glucuronide	$C_{25}H_{33}NO_{13}$	556.2030	2.26, 2.81	13.06±3.42[##]	0.30±0.03
Others					0.47±0.18	0.68±0.05[*]

Fig. 1

A

B

Fig. 2

Fig. 3

XXXIX and XXXX **XXIV to XXVI** **X** **XVII and XVIII** **XXX to XXXII**

XXXIII and XXXIV **III** **II** **VI** **VII**

XIX and XX **XI** **Cocaine (I)** **V** **IV**

XXVII and XXVIII **XIII and XIV** **XII** **IX** **VIII**

XXXXI and XXXXII **XXI to XXIII** **XXXV to XXXVIII** **XV and XVI** **XXIX**

Fig. 4

Fig. 5

Fig. 6